Bioconjugate Chemistry

pubs.acs.org/bc Article

New Generation Oxyntomodulin Peptides with Improved Pharmacokinetic Profiles Exhibit Weight Reducing and Anti-Steatotic Properties in Mice

Peng-Yu Yang,[§] Huafei Zou,[§] Zaid Amso,[§] Candy Lee, David Huang, Ashley K. Woods, Vân T. B. Nguyen-Tran, Peter G. Schultz,* and Weijun Shen*

Cite This: https://dx.doi.org/10.1021/acs.bioconjchem.0c00093 Read Online

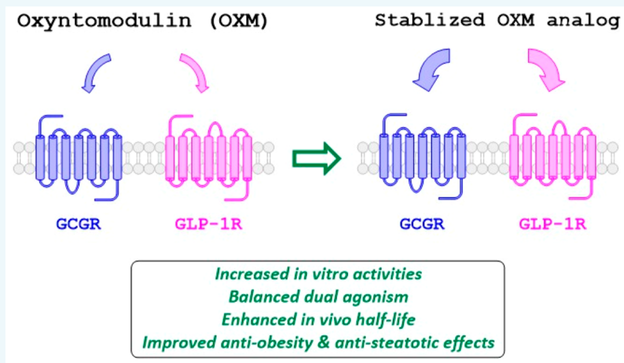

ABSTRACT: Oxyntomodulin (OXM) is an intestinal peptide hormone that activates both glucagon-like peptide-1 (GLP-1) and glucagon (GCG) receptors. The natural peptide reduces body weight in obese subjects and exhibits direct acute glucoregulatory effects in patients with type II diabetes. However, the clinical utility of OXM is limited due to its lower *in vitro* potency and short *in vivo* half-life. To overcome these issues, we developed stapled, long-acting, and highly potent OXM analogs with balanced activities at both GLP-1 and GCG receptors. The lead molecule **O14** exhibits potent and long-lasting effects on glucose control, body weight loss, and reduction of hepatic fat reduction in DIO mice. Importantly, **O14** significantly reversed hepatic steatosis; reduced liver weight, total cholesterol, and hepatic triglycerides; and improved markers of liver function in a nonalcoholic steatohepatitis (NASH) mouse model. A symmetrical version of the peptide was also shown to be more efficacious and long-lasting in controlling glucose than semaglutide and the clinical candidate cotadutide in wild-type mice, highlighting the utility of our designs of the dual agonist as a potential new therapy for diabetes and liver diseases.

■ INTRODUCTION

Obesity is known to be a strong risk factor for type 2 diabetes (T2D), fatty liver disease, cardiovascular disease, and cancer. In fact, 85% of patients with diabetes are overweight or obese. Moreover, modest weight loss can prevent the onset of T2D in the overweight or obese, and lead to a reduced requirement for anti-hyperglycemic drug therapy in those with established T2D. However, attempts to develop safe and effective medical treatments for obesity have had limited success, and several drugs have been withdrawn due to serious adverse effects.[1] Bariatric surgery, such as gastric bypass, is currently considered the most effective treatment for severely obese patients, which results in successful long-term, sustained weight loss. After bariatric surgery, T2D patients have shown a significant improvement in glycemic control, even before substantial weight loss, and often discontinue medication for diabetes control.[2] It is now well-established that following gastric bypass, there is a significant alteration in the secretion of various gut hormones including glucagon-like peptide-1 (GLP-1), peptide YY (PYY), glucose-dependent insulin-tropic peptide (GIP), oxyntomodulin (OXM), and fibroblast growth factors (FGFs) that are associated with glucose homeostasis, appetite, and satiety, as well as energy expenditure through modulation of peripheral target organs.[3] Accordingly, unimolecular combinatorial hormones aimed at mimicking endogenous signals that occur after bariatric surgery to promote weight loss and simultaneously improve glucose metabolism have emerged as new treatment options for people with obesity and T2D.[4−8]

GLP-1 targets the pancreas and CNS to induce insulin secretion and satiety, which has led to regulatory approval of several GLP-1-based therapies for the treatment of T2D.[9] However, these GLP-1R agonists offer modest weight loss in most obese patients that is limited by a dose-dependent increase in adverse GI effects, as exemplified by Saxenda (liraglutide 3 mg/day).[10,11] Notably, recently approved once-weekly *s.c.* semaglutide for the treatment of T2D demonstrated superior weight loss efficacy in a phase II dose-finding trial when compared with both placebo and liraglutide in patients with obesity but without T2D.[12]

Glucagon receptor (GCGR) agonism has also been shown to exert effects on lipid metabolism, energy balance, body

Received: February 17, 2020
Revised: March 23, 2020

adipose tissue mass, and food intake.[13,14] Activation of GCGR is classically associated with an elevation in glucose levels, which would be deleterious in T2D patients, but the antidiabetic properties of GLP-1R agonism would be expected to counteract this effect. Indeed, coadministration of native GLP-1 and glucagon decreases food intake while increasing energy expenditure without any detectable adverse effects in humans.[15,16]

OXM, a 37-amino-acid peptide hormone derived from proglucagon, is an endogenous hormone that activates both GLP-1R and GCGR, albeit with 10- to 100-fold lower potency compared with native GLP-1 and glucagon.[17,18] OXM administration improved glucose tolerance in diet-induced insulin-resistant mice, and recently, the same effect were observed in T2D patients.[19,20] Moreover, two independent groups have recently reported that GLP-1R/GCGR dual agonists led to increased weight loss relative to pure GLP-1R agonists in obese rodents and nonhuman primates, with simultaneous improvement in glycemic control.[21−23] Preclinical studies indicated the importance of proper balance of agonist activities on both receptors to achieve maximum metabolic benefits,[24] although this notion is still being tested in human clinical settings, including HM12525A (Hanmi Pharmaceuticals/Janssen), MEDI-0382 (AstraZeneca), and SAR425899 (Sanofi).[25−27]

More recently, it has been shown that subcutaneous OXM causes weight loss in overweight and obese healthy subjects, and appears well-tolerated.[20,28,29] However, the half-life of OXM is very short (∼10 min);[30] therefore, repeated daily administration of supra-physiological doses are required to achieve a pharmacological effect in humans, which limits its clinical utility. Several groups have recently developed dipeptidyl peptidase IV (DPP-IV)-resistant OXM analogs with similar *in vitro* potencies to native OXM but prolonged *in vivo* activity in mice, suitable for once-daily administration.[31−37] Although PEGylation extends the duration of action of OXM for potentially once-weekly dosing exemplified by once-weekly pegapamodutide and MOD-6031, the resultant analogs suffer from reduced potency and, as a result, require higher doses to be effective.[22,38−40] We have previously shown that incorporation of a serum protein binding motif into a covalent cysteine (Cys) α helix staple can significantly improve the pharmacokinetic (PK) profile of exendin-4 (Ex-4) and teduglutide.[41−43] Herein, we extend this approach to generate a balanced OXM analog with high potencies on both receptors, and enhanced half-life compared to the native hormone OXM. The lead molecule demonstrates excellent efficacy in both body weight reduction and metabolic control in DIO mice. Furthermore, it also shows superior anti-steatotic effect in choline deficient NASH rodent model.

RESULTS AND DISCUSSION

Stapled Peptide Design and *in Vitro* Receptor Agonist Activity. Accumulating evidence indicates that α-helical conformations of GLP-1 and GCG may be required for binding to their target receptors.[44,45] OXM contains a C-terminal extension of glucagon and also exhibits high sequence homology to GLP-1. Based on the homology model of OXM bound to the N-terminal extracellular domain of GLP-1R, we have previously identified an optimal di-Cys-containing OXM sequence (SEQ-1, Figure 1A), and shown that stapling OXM with a biaryl cross-linker at i and i + 7 positions enhances the peptide's helicity and improves potency and half-life, when compared to the linear counterpart.[46] We reasoned that introduction of lipid-modified linkers (e.g., L2−L5, Figure 1B) could further enhance the pharmacokinetic (PK) properties of these peptides through binding to circulating serum proteins.

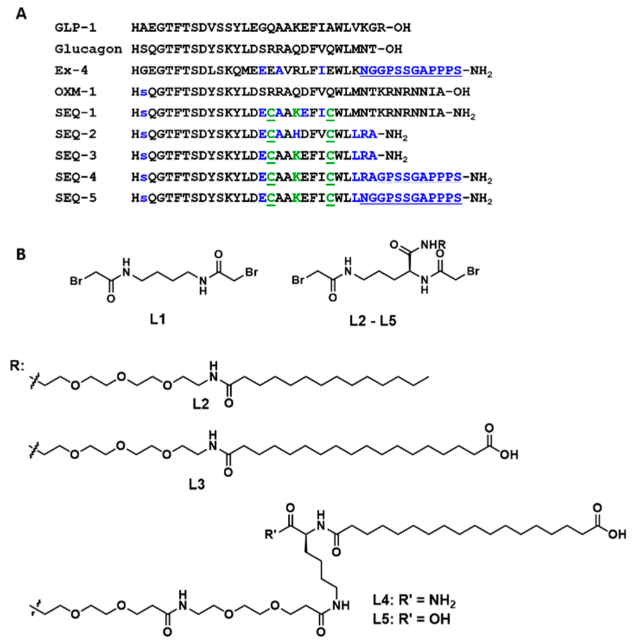

Figure 1. Design of stapled OXM analogs. (A) Sequence alignment of GLP-1, glucagon, Ex-4, OXM, and double Cys mutants spaced at i, i + 7. (B) Structures of lipidated cross-linkers containing Cys-reactive bis-bromoacetamide moiety.

To test this notion, SEQ-1 peptides were cross-linked with the linkers L1, L2, and L3 (in 30 mM aq NH_4HCO_3/CH_3CN 3:1) to generate a series of stapled peptides **O1−O3**, respectively, in >50% overall yield after HPLC purification. The first staple L1 lacks a fatty acid moiety and was used as a reference linker for comparison purposes. Staple L2 features three ethylene glycol units terminating in a myristoyl group, while L3 also has three ethylene glycol units but with a terminal octadecanedioic acid moiety. The presence of the longer chain fatty acid (C_{18}) in the L3 staple can offer an enhanced binding affinity to albumin, when compared to the L2 staple.[37,43] Additionally, the terminal carboxylate in L3 is predicted to interact with basic residues in albumin, thereby delivering a higher impact on the binding affinity and consequently *in vivo* half-life.[47,48] L4 comprises four ethylene glycol units attached to octadecanedioic acid via a lysine linker incorporating an internal carboxylate moiety terminating in a myristoyl group, while L5 carries a similar structure to L4 with the replacement of the internal carboxylate with an amide functional group. The chemical stucture of L4 is similar to the lipid protractor used for semaglutide, which exhibits favorable binding to human serum albumin. Such a modification enhances semaglutide's half-life, which renders the peptide suitable for once-weekly administration.

The agonistic activity of these peptides was determined using a cAMP response element (CRE)-driven luciferase reporter in HEK293 cells stably expressing human GLP-1R and GCGR. Ex-4 and glucagon were used as positive controls. As expected, the conformationally restricted **O1** (L1; EC_{50} = 0.03 nM for GLP-1R and 0.2 nM for GCGR, Table 1) shows >300- and ∼15-fold higher potency in GLP-1R and GCGR activation, respectively, compared to the DPP-IV resistant

Table 1. Summary of the *in Vitro* Potency of Stapled Peptides in Human GLP-1R- and GCGR-Mediated CRE-Luc Reporter Assays[a]

Name	SEQ	Linker	EC_{50} (nM) GLP-1R	EC_{50} (nM) GCGR
Ex-4			0.02	
GCG				0.068
Semaglutide			0.05	
OXM-1			10	3
SEQ-1			17	30
SEQ-3			5.2	9.2
O1	SEQ-1	L1	0.03	0.2
O2	SEQ-1	L2	0.04	0.3
O3	SEQ-1	L3	2.0	3
O4	SEQ-2	L1	0.2	0.04
O5	SEQ-2	L2	0.1	0.1
O6	SEQ-3	L1	0.03	0.03
O7	SEQ-3	L2	0.03	0.05
O8	SEQ-3	L3	0.03	0.1
O9	SEQ-3	L4	0.05	0.5
O10	SEQ-3	L5	0.3	1.0
O11	SEQ-4	L3	0.04	0.4
O12	SEQ-4	L4	0.3	0.5
O13	SEQ-4	L5	0.5	1
O14	SEQ-5	L3	0.03	0.15
O15	SEQ-5	L4	0.04	0.3
O16	SEQ-5	L5	0.04	0.4

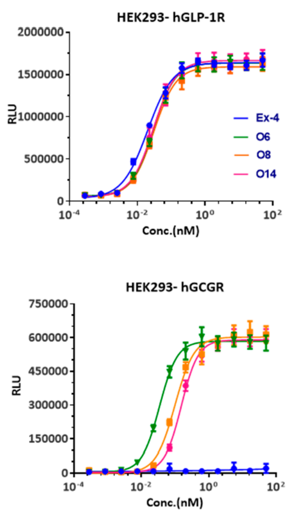

[a]The potency of representative peptides are shown in comparison with EX-4. EC_{50} values for activation of GLP-1R and GCGR determined using HEK293 cells overexpressing GLP-1R and GCGR, respectively, carrying a cAMP response element (CRE) luciferase (Luc) reporter. The assay was performed in triplicate.

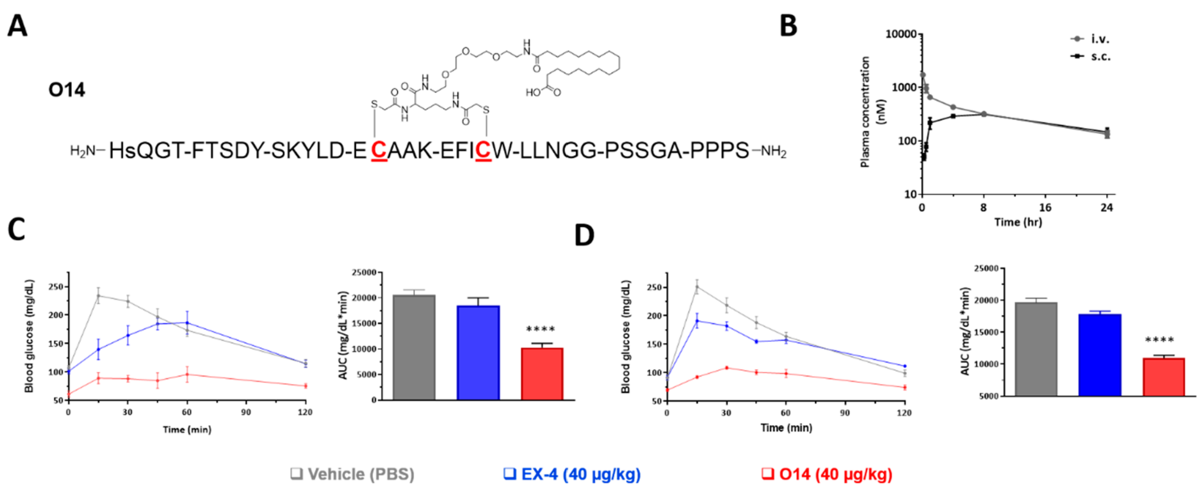

Figure 2. Characterization of stapled OXM analog **O14**. (A) Structure of **O14**. (B) Pharmacokinetic profiles of **O14** in mice. **O14** (40 μg/kg) in PBS (pH 8.1) was administered by *i.v.* or *s.c.* injection into CD1 mice (n = 4 per group). Blood samples were collected at the indicated time points and analyzed by *in vitro* GLP-1R activity assay. The assay was performed in triplicate. Pharmacokinetic analyses were determined by noncompartmental analysis with WinNonLin. (C) OGTT in normal mice. Plasma glucose levels during OGTT in normal mice treated by *i.v.* (C) or *s.c.* (D) injection. CD1 female mice (n = 5 per group) were injected with vehicle, **O14** (40 μg/kg), or Ex-4 (40 μg/kg) for 6 h prior to the glucose challenge. Bar graph shows the levels of glucose in mice obtained by measuring the area under the curve (AUC). Data are means and SE, n = 5 per group. $^{**}P < 0.001$ (one-way ANOVA test) vs PBS-treated mice.

OXM, OXM-1 (OXM with D-serine at the second position). To our satisfaction, **O2** (L2; EC_{50} = 0.04 nM for GLP-1R and 0.3 nM for GCGR, Table 1) exhibited only a 2- and 4.5-fold decrease in agonist potency at GLP-1R and GCGR, respectively, compared to Ex-4 and glucagon. Additionally, the stapled peptide displayed improved *in vitro* plasma stability over exenatide (EX-4) and extended *in vivo* half-life (>3 h) in mice, suitable for once daily dosing in humans (Figure S1, Supporting Information). However, cross-linking SEQ-1 with linker L3, which may have a higher affinity to albumin based on a previous study,[37] resulted in analog **O3** with 10- and 45-fold loss of potency at GLP-1R and GCGR, respectively.

To obtain potent OXM analogs with higher affinity for albumin that are potentially suitable for once-weekly administration, without compromising the potency relative to native GLP-1 and glucagon, we explored other OXM variants with modified sequences. The structure of SEQ-3 and SEQ-4 lacks the C-terminal residues of OXM. To prevent potential oxidation reactions, SEQ-3 and SEQ-4 features a subsititution of Met(27) from the OXM sequence with Leu. Also included is Arg at position 28, a key binding residue from liraglutide, a once-daily therapy for T2D. By stapling with the different ethylene glycol−fatty acid moieties, peptides **O4**−**O10** were generated, which showed a significant increase in potency compared to the corresponding non-cross-linked peptides (Table 1). A significant drawback of these peptides was their insufficient solubility properties in aqueous conditions; thus, their *in vivo* efficacies could not be tested. Additionally, LC-MS

https://dx.doi.org/10.1021/acs.bioconjchem.0c00093
Bioconjugate Chem. XXXX, XXX, XXX−XXX

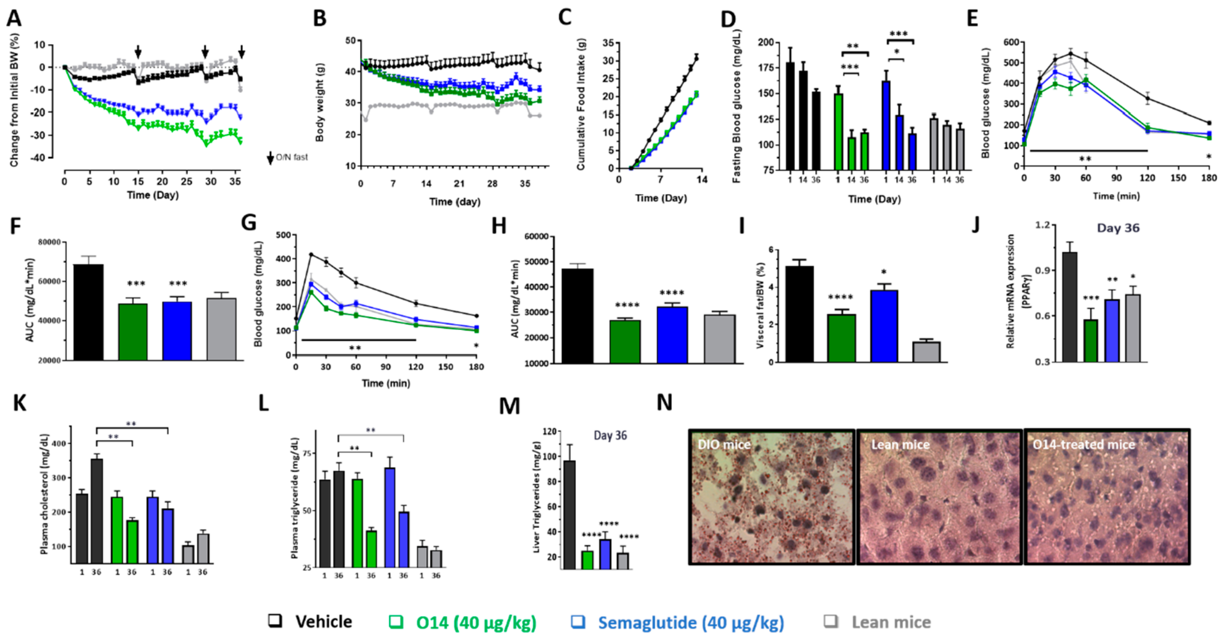

Figure 3. *In vivo* efficacy of **O14** in DIO mice treated for 5 weeks. Effects on body weight change (A), crude body weight (B), cumulative food intake (C), fasted blood glucose on days 15 and 36 (D), OGTT on day 15 (E,F), IPGTT on day 36 (G,H), visceral mass change (I); PPARγ mRNA levels in brown fat (J), plasma cholesterol (K), plasma triglycerides (L), and liver triglycerides (M) of lean and DIO mice on day 36. (N) Representative hematoxylin and oil red O staining of liver sections of DIO and lean mice at the end of the treatment (two images per mouse), Scale bars, 100 μm. C57BL/6 mice (male, 6 weeks old) were treated with PBS (*s.c.*, once daily), **O14** (*s.c.* once daily) for 35 days. The arrows indicate time of fasting for glucose tolerance test. Data are means ± SE, n = 9 per group. $^{**}P$ < 0.001 (one-way ANOVA test) vs PBS-treated mice.

analysis of these peptides indicated the presence of two inseparable peaks, resulting from the asymmetrical nature of the fatty acid linker employed in our experiment (Figures S3 and S5, Supporting Information). To improve the solubility, OXM chimeric double Cys mutants SEQ-4 and SEQ-5 were generated that incorporate key binding residues from Ex-4, namely, the addition of the 12 C-terminal residues of Ex-4 to a C-terminal truncated OXM (SEQ-4 and SEQ 5). SEQ-5 features the substitution of Arg(28) with Asn, resulting in an improvement in the GLP-1R agonism potency. Fruitfully, stapled peptide **O14**, containing the fatty acid moiety L3, showed the desired balance in the activation of the two receptors, with comparable activity relative to Ex-4 at GLP-1R, and less than a 2-fold decrease in potency relative to glucagon at GCGR (Table 1). LC-MS analysis of **O14** presented the peptide as a single peak, which may comprise an inseparable mixture of two isomers (Figure S7, Supporting Information).

Next, we determined the α-helicity of three representative potent stapled peptides (**O6**, **O8**, and **O14**) by circular dichroism (CD) using OXM-1 as a positive control. At room temperature, the CD spectrum of the stapled peptides exhibited a significant increase in helicity as compared to OXM-1 (Figure S2, Supporting Information). In particular, **O8** showed the greatest increase in the helicity, followed by **O14** and finally **O6**, indicating that that lipidation can also stabilize helical structure and modify biological function, as previously shown.[41] Based on the potency, solubility, and the helical nature, the stapled peptide **O14** was chosen as the lead candidate for *in vivo* experiments.

Pharmacokinetics and Oral Glucose Tolerance Test (OGTT) in Wild-Type Mice. To determine the *in vivo* half-life of the potent analog **O14**, pharmacokinetic (PK) studies were performed in CD1 female mice by *i.v.* or *s.c.* injection of the peptide at 40 μg/kg. The plasma level of the peptide at indicated time points was determined using the *in vitro* GLP-1R reporter assay. The estimated terminal half-life after *i.v.* administration is 6 min for OXM-1 and 8.3 h for **O14**. Plasma OXM-1 became undetectable after 1 h from its administration (<10 nM), whereas **O14** exhibited higher T_{max} and C_{max} (8 h and 300 nM, respectively) after *s.c.* administration (Figure 2B). Notably, the terminal mouse plasma half-life of **O14** is similar to that of semaglutide (rodent half-life is ~8 h),[49] which has been clinically approved for once-weekly application in T2DM patients. It is also noteworthy that, although our focus for half-life extension was on the serum-binding ability of the stapled peptide, there may be a combination of effects, for example, self-assembly and depoting at the injection site, that led to the delayed onset of C_{max} and the extended half-life, and thus the individual contribution of these factors is worth investigating further in the future.

To examine the glucose-lowering effect of the optimal peptide **O14** in comparison to EX-4, the peptides (at 40 μg/kg) were administered as single doses intravenously or subcutaneously to CD1 female mice 6 h prior to the glucose challenge. Due its short half-life, Ex-4 partially decreased blood glucose levels, as determined by the oral glucose tolerance test (OGTT), at the time points of 15 and 30 min after the 6 h period. On the other hand, the stapled peptide **O14** markedly decreased blood glucose levels during the entire monitoring period, an effect that is consistent with the peptide's extended *in vivo* half-life in comparison to EX-4 (Figure 3C and D).

O14 Decreased Body Weight and Improved Glucose Intolerance and Dyslipidemia and Attenuated Hepatic Steatosis in DIO Mice. Encouraged by the preliminary PK and PD results, we then assessed the efficacy of chronic administration of **O14** in a high-fat-diet-induced obesity (DIO) mouse model. DIO mice (C57BL/6, male, 25 weeks old) were randomized based on their body weight and then

https://dx.doi.org/10.1021/acs.bioconjchem.0c00093
Bioconjugate Chem. XXXX, XXX, XXX−XXX

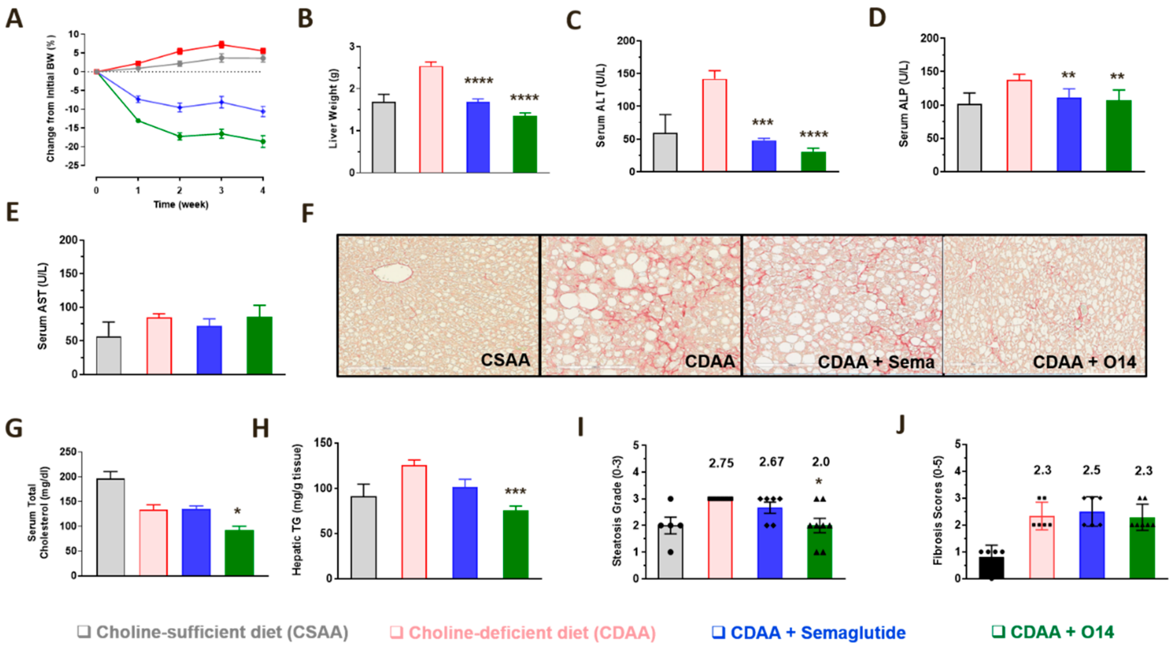

Figure 4. Chronic treatment of semaglutide and **O14** in CDAA-induced NASH mice. Effects on body weight change (A), liver weight (B), serum ALT (C), ALP (D), and AST (E). (F) Liver steatosis and fibrosis are analyzed by picrosirius red and H&E staining. Representative images are shown, and histopathological evaluations were conducted using a semiquantitative scoring system. Scale bars, 200 μm. Also presented here are serum cholesterol (G), hepatic triglycerides (H), along with the steatosis (I) and fibrosis (J) scores. C57BL/6 mice (male, 5 weeks old) were maintained on choline-deficient L-amino acid (CDAA) 40% fat diet. After 12 weeks of diet induction, mice were randomized based on serum ALT, AST, and body weight into treatment groups. Mice were treated daily with either vehicle (saline) or compound for 4 weeks. Data are means ± SE, n = 9 per group. **$P < 0.001$ (one-way ANOVA test) vs vehicle-treated mice.

treated for 5 weeks by *s.c.* dosing of PBS, **O14** (40 μg/kg), or semaglutide (40 μg/kg; positive control). Wide-type lean mice were used as normal controls.

Fruitfully, **O14**-treated DIO mice exhibited a steady reduction in body weight and fasting blood glucose levels, with a profile similar to that of the semaglutide-treated group (Figure 3A,B). At an efficacious dose of 40 μg/kg, **O14** significantly reduced body weight by 27.3 ± 1.3% and 33.5 ± 1.7% (vs baseline) at days 14 and 36, respectively. Although this weight loss appeared to be parallel to a robust reduction in food intake (Figure 3C), other GCGR-driven mechanisms, such as increased energy expenditure, thermogenesis, and endogenous circulating FGF21, may have also contributed to this dramatic weight loss effect.[50,51] The effects on body weight were also examined for a higher concentration (120 μg/kg) of **O14** and revealed a more significant reduction, reaching the body weight level of lean mice after only 2 weeks. Due to concerns over extreme body weight loss with ongoing treatment, administration of the higher dose was terminated. Notably, 2 weeks after treatment cessation for the high-dose **O14** subgroup, body weight rebounded to levels comparable to that of vehicle-treated controls (data not shown), suggesting that the peptide does not cause irreversible toxicity in DIO mice. Moreover, to assess any toxicity associated with the observed weight reduction, we performed hematology and blood chemistry and did not observe any obvious differences between the high-dose and PBS groups.

Apart from a reduction in fasting blood glucose levels, in an OGTT on day 15 and IPGTT on day 36, the levels of blood glucose in **O14**-treated DIO mice were similar to those in the lean mice group, and significantly lower compared to PBS-treated DIO mice (Figure 3D−H). In addition, determination of body composition indicated that the decrease in body weight was also associated with a reduction in fat mass (Figure 3I). This was further corroborated by a significant decrease in the PPARγ mRNA levels in fat, as quantified by real-time RT-PCR (Figure 3J). We also observed favorable changes in lipid metabolism including triglycerides and cholesterol in liver and plasma. Indeed, **O14** treatment resulted in decreased plasma cholesterol levels (177 ± 7 mg/dL, compared to PBS-treated 355 ± 14 mg/dL) and reduced triglyceride levels in both plasma and liver (41 ± 1 and 21 ± 2 mg/dL, respectively) relative to PBS treatment (67 ± 3 and 97 ± 13 mg/dL, respectively) (Figure 3K−M). Finally, chronic treatment with **O14** resulted in a decreased hepatic steatosis, as demonstrated by a marked reduction in hepatic lipid content in the livers of **O14**-treated DIO mice (Figure 3N). Indeed, no difference was observed in the liver lipid accumulation of **O14**-treated DIO mice vs lean control mice. Accordingly, these results suggest that **O14** could offer a potential clinical benefit for the treatment of fatty liver diseases such as nonalcoholic fatty liver disease (NAFLD) and nonalcoholic steatohepatitis (NASH).[36,52,53]

O14 Reversed Advanced NASH More Potently than Semaglutide in Mice. Having shown excellent efficacy in a DIO mouse model, our next goal was to evaluate the effects of stapled peptide **O14** on liver fibrosis in a nutrient-deficient dietary model. The choline-deficient, L-amino acid-defined (CDAA) diet was utilized for our mouse model, as it can induce liver injury (increase hepatic enzymes) and induce mild to moderate fibrosis in relatively shorter time (13−16 weeks) of diet induction compared to conventional obesogenic diets with high variability and up to 30% nonresponders.[54] Also, this model has been demonstrated to mimic human NASH by sequentially producing steatohepatitis, liver fibrosis, and liver cancer without any loss of body weight.[55]

https://dx.doi.org/10.1021/acs.bioconjchem.0c00093
Bioconjugate Chem. XXXX, XXX, XXX−XXX

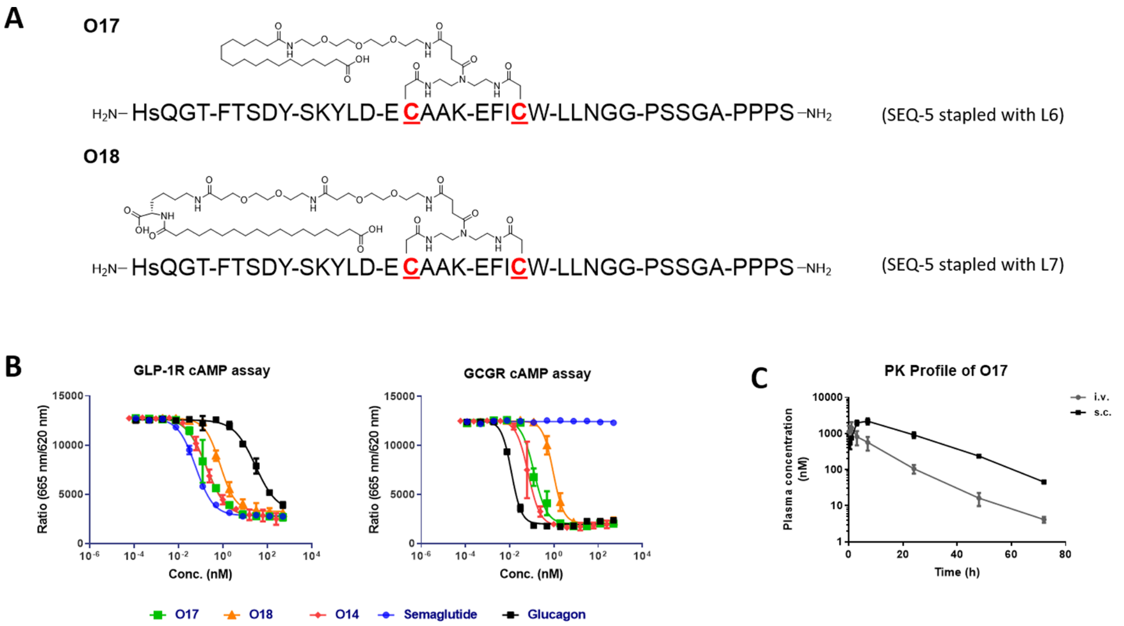

Figure 5. Structure−activity relationship of the second generation stapled. (A) Structures of **O17** and **O18**. (B) *In vitro* activity of the stapled peptides in cells overexpressing GLP-1R and GCGR, respectively, compared to semaglutide and glucagon. (C) Pharmacokinetic profiles of **O17** in mice. Peptide in PBS (pH 8.1) was administered by *i.v.* (concentration of 0.3 mg/kg) or *s.c.* (1.0 mg/kg) injection into CD1 mice ($n = 4$ per group). Blood samples were collected at the indicated time points and analyzed by *in vitro* GLP-1R activity assay. The assay was performed in triplicate. Pharmacokinetic analyses were determined by noncompartmental analysis with WinNonLin.

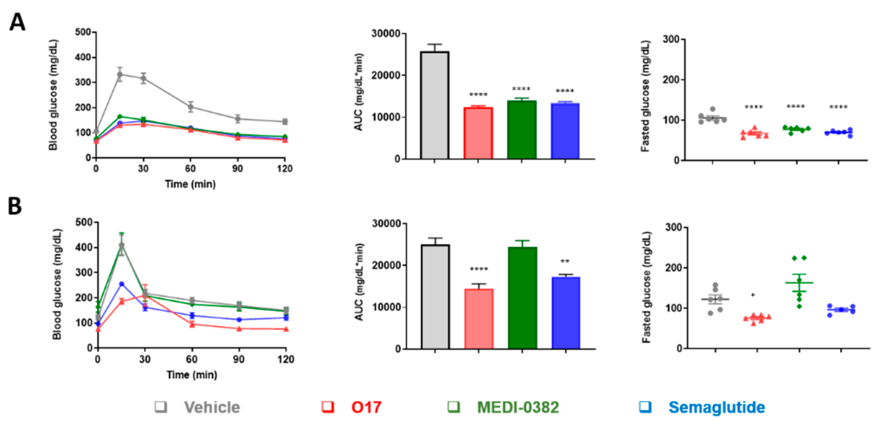

Figure 6. Plasma glucose excursion during OGTT in normal mice after 6 h (A) and 48 h (B) post-injection. CD1 female mice ($n = 6$ per group) were *s.c.* injected with vehicle, **O17**, MEDI-0382, or semaglutide (at 40 μg/kg each), 6 h prior to the glucose challenge. Bar graph shows the levels of glucose in mice obtained by measuring the area under the curve (AUC). Effects on fasted blood glucose are also reported here. Data are means and SE, $n = 6$ per group. ****$P < 0.0001$; **$P < 0.005$; *$P < 0.05$ (one-way ANOVA test) vs PBS-treated mice.

Mice were placed on either choline-deficient diet or AA supplemented control diet for a total of 16 weeks. **O14** (40 μg/kg) was then administered to mice daily for the final 4 weeks, and its efficacy was compared to semaglutide, currently in Phase II clinical trials for treating NASH and a vehicle control. The choline-supplemented L-amino acid (CSAA) diet mice were also fed as the control diet does not induce the NASH phenotype. After 4 weeks of treatment, administration of either **O14** or semaglutide triggered significant reduction of body weight ($p < 0.005$ for semaglutide vs $p < 0.0001$ for **O14**) and liver weight, as well as improvements in markers of liver function (ALT and ALP) (Figure 4A−E). Histologically, **O14** treatment markedly ameliorated macrovascular steatosis and fibrosis (Figure 4F). To our satisfaction, mice treated with **O14** exhibited improvements over the semaglutide-treated group in the levels of total cholesterol and hepatic triglycerides (Figure 5G and H). Furthermore, steatosis, but not fibrosis, was significantly reduced in the **O-14**-treated animals in comparison to those treated with semaglutide or a vehicle control (Figure 4I and J). Together, these results suggest that **O14** results in improvements in liver function and efficacy in reversing steatosis to levels that are more significant than semaglutide, potentially due to its dual agonism effects.

Using Symmetrical Linkers to Control the Identity of the Final Stapled Peptide. Despite the high potency and efficacy of **O14**, its linker is structurally asymmetric, and it is currently unknown how geometric variations of this stapled peptide affect bioactivity and interaction with the targeted receptors. Additionally, it is extremely difficult to identify which of the two stapled variants corresponds to the right molecule that elicited the reported pharmacological effects. To circumvent this issue, second-generation serum-binding linkers

https://dx.doi.org/10.1021/acs.bioconjchem.0c00093
Bioconjugate Chem. XXXX, XXX, XXX−XXX

were developed (L6 and L7) and incorporated *via* thioether linkages into SEQ-5 to produce **O17** and **O18** (Figure 5A). To reflect the true affinity toward their targeted receptors, **O17** and **O18** along with **O14** were tested in the absence of serum using a CHOK-1 cells overexpressing human GLP-1R or GCGR. Fruitfully, peptide **O17** with a symmetrical linker exhibited a similar potency to the asymmetric **O14** on both GLP-1R and GCGR (Figure 5B) and was therefore chosen as the new lead design for our next *in vivo* experiments.

The terminal half-life of **O17** after a single dose was approximately 10.1 h in mice (Figure 5C). The PK profile was also characterized by significantly reduced clearance value (3.61 mL/h/kg). These results show that, similar to the asymmetric **O14**, the plasma half-life of **O17** in mice is similar to or better than that of semaglutide (around 8 h).[37]

The efficacy of the GLP-1R/GCGR dual agonist **O17** was then evaluated in an oral glucose tolerance test (OGTT) in wild-type mice. As positive controls, we employed the once-weekly administered, single GLP-1R agonist semaglutide and the dual GLP-1R/GCGR agonist MEDI-0382, a once-daily administered peptide currently in Phase II trials by AstraZeneca. All peptides significantly decreased blood glucose to a similar level 6 h post-administration when compared to the vehicle (Figure 6a). Similar results were observed for fasted blood glucose for all peptides. However, significant differences in glucose levels were observed after 48 h from administration of the peptides. MEDI-0382 did not exhibit any improvement over the vehicle after 48 h, consistent with its suitability as a once-daily injection for human subjects. On the other hand, mice treated with **O17** showed more significant improvements in handling glucose after 48 h compared to semaglutide (Figure 6b). Moreover, **O17** was able to significantly reduce fasted glucose levels, while the rest of the peptides resulted in no improvements in efficacy. The increased *in vivo* efficacy of **O17** observed here likely resulted from both higher dual agonistic activity and the extended *in vivo* half-life. Assuming a direct relationship between pharmacokinetics and pharmacokinetics, the results of this experiment indicate that peptide **O17** exhibits a longer half-life than semaglutide, and thus has the potential to be developed as a once-weekly or semimonthly with an appropriate formulation. The efficacy of **O17** is currently being evaluated in more complex preclinical models of diabetes and fatty liver diseases, and results will be reported in the near future.

■ CONCLUSIONS

In summary, we have demonstrated that long-acting OXM analogs can be generated by incorporating a serum protein binding motif into a di-Cys staple. One of the lead peptides, **O14**, shows balanced dual activation of GLP-1 and glucagon receptors and comparable potency to the native hormones with extended half-life in rodents. Further, **O14** exhibited potent effects on glucose control, body weight loss, and reduction of hepatic fat reduction in DIO mice. Notably, **O14** treatment significantly reversed hepatic steatosis and reduced cholestrol and hepatic triglyceride levels in NASH mice compared to semaglutide treatment. We also report a new design of symmetrical stapled peptides, one of which exhibited a potent GLP-1R/GCGR dual agonist potency, long half-life, and improved *in vivo* efficacy over semaglutide in wild-type mice. These improvements in pharmacokinetics and pharmacodynamics support that our long-acting OXM analog has the therapeutic potential as a weight loss, anti-diabetic, and anti-steatotic agent. This same approach is likely to be applicable to other endogenous peptides such as PYY and dual GLP-1/GIP receptor agonists.

■ EXPERIMENTAL PROCEDURES

Peptide Cross-Linking. The dicysteine-containing peptide (2 mM, >95% pure) (InnoPep, San Diego, CA) and the cross-linker (1.5 equiv) were dissolved in CH_3CN/30 mM NH_4HCO_3 buffer (v/v; 1:3) pH 8.5), and the reaction was stirred at room temperature for 2−4 h. Under ice cooling, acetic acid was then added dropwise to reduce the pH of the mixture to around 5 and the crude cross-linked peptide was then purified by preparative HPLC column (Phenomenex, 5 μm C_{18}, 300 Å, 50 × 250 mm) with a linear gradient from 20% to 80% CH_3CN/H_2O containing 0.05% trifluoroacetic acid for 30 min at a flow rate of 15 mL/min. The fractions containing the products were collected and lyophilized to afford the products as a powder with >95% purity and in >50% product yield.

The identity of the purified peptide was confirmed by ESI-MS. Analytical HPLC was performed using an Agilent 1100 series LC/MS system with a ZORBAX C_{18} column (5 μm, 150 × 4.6 mm) from Agilent with a linear gradient of 10−70% CH_3CN/H_2O containing 0.1% formic acid for 20 min at a flow rate of 1.0 mL/min with UV−Vis detection wavelength set at 214 nm.

Generation of CRE-Luc Stable Cell Line Overexpressing GLP-1R or GCGR. HEK293 cells were infected with lentivirus encoding firefly luciferase genes under the control of cAMP responsive element (CRE) promoter (Qiagen, The Netherlands) and then were selected using 1 μg/mL puromycin (Life Technologies, Carlsbad) for 1 week. The surviving cells (referred to as CRE-HEK293) were expanded and then transfected with a G418 selective mammalian expression plasmid encoding human GLP-1R or GCGR. In brief, GLP-1R or GCGR plasmid was transfected into CRE-HEK293 cells using Lipofectamine 2000 and selected with 400 μg/mL Geneticin (Life Technologies, Carlsbad, CA). Single colony stable cell line overexpressing CRE-luciferase and GLP-1R or GCGR (HEK293-GLP-1R-CRE or HEK293-GCGR-CRE) was then established for *in vitro* activity assay.

***In Vitro* Receptor Activation Reporter Assay (Receptor-Mediated cAMP Synthesis).** HEK293-GLP-1R-CRE or HEK293-GCGR-CRE cells were seeded in 384-well plates at a density of 5000 cells per well and cultured for 18 h in DMEM with 10% FBS at 37 °C and 5% CO_2. Cells were treated with peptides in a dose-dependent manner for 24 h, and receptor activation was reported by luminescence intensities, using One-Glo (Promega, WI) luciferase reagent following manufacturer's instruction. The EC_{50} of each peptide was determined using GraphPad Prism 6 software (GraphPad, San Diego, CA).

cAMP Assay. CHOK1 cells stably overexpressed human GLP-1R or GCGR (20 μL of 5000 cells per well) were seeded in a white solid 384 well plate covered with metal lid and incubated overnight. On day 2, the culture medium was replaced by fresh medium containing no FBS (for 0% FBS group). Cells were treated with 5 μL peptide in 12-point dose response, in culture medium with 0.5 mM IBMX in triplicate for 30 min at 37 °C, 5% CO_2. cAMP dynamic 2 kit from Cisbio was used to detect cAMP level. Briefly, 25 μL of cAMP detection reagent (1:1:38 of cAMP-d2, Cryptate conjugate, lysis buffer) per well was added and incubated at room temperature for 1 h. For cell negative control wells, cAMP detection reagent without d2 was added. Plates were then read at Ex320 nm, Em-1 665 nm, and Em-2 620 nm. Graphs were plotted with Ratio or Delta F using Prism software, and EC_{50} values were then obtained. Ratio = $A_{665\ nm}/B_{620\ nm} \times 10^4$. %$\Delta F$ = (Standard or Sample Ratio − $Ratio_{neg}$)/$Ratio_{neg}$ × 100.

Animals. Animal care and experimental procedures were approved by the Institutional Animal Care and Use Committee (IACUC) of Calibr at the Scripps Research Institute, strictly following the NIH guidelines for humane treatment of animals.

Pharmacokinetics of Peptides in Mice. Female CD-1 mice (n = 4 per group) from Charles River Laboratory were fasted overnight and administered 100 μL of each peptide in phosphate buffered saline by intravenous (*i.v.*) or subcutaneous (*s.c.*) route. Food was provided to mice after blood collection at 3 h time point. Blood was collected into heparin tubes and centrifuged at 3000×g for 15 min. The resulting plasma were then stored at −80 °C for peptide concentration determination. The concentrations of peptides in plasma at each time point were determined by *in vitro* cell based activity assay. Briefly, HEK293-GLP-1R-CRE cells were treated with plasma samples at different time points (5-point dose response, starting from 1:10 to 1:100 dilution of each plasma sample) and incubated for 16 h in DMEM with 10% FBS at 37 °C with 5% CO_2, and the firefly luciferase activity was then measured. Simultaneously, the same peptides were used to obtain standard curves and parameters for Bottom, Top, EC_{50}, and Hill Slope. Relative luciferase unit (RLU) for each plasma sample was used to calculate the peptide concentrations in plasma (nmol/L), using parameters derived from the standard curve (RLU = Bottom + (Top − Bottom)/(1 + $10^{(\mathrm{LogEC_{50}\text{-}conc.}) \times \mathrm{Hill\ Slope}}$). Peptide concentrations in plasma were obtained and plotted against time points to obtain *in vivo* half-life of each peptide, using WinNonLin Phoenix software (Pharsight Corp, St. Louis, MO).

Oral Glucose Tolerance Test (OGTT)/Intraperitoneal Glucose Tolerance Test (IPGTT). Female Charles River CD-1 mice were fasted overnight and then administered 100 μL of each peptide in PBS (pH = 8.1) by *i.v.* or *s.c.* route. After 6 h, mice were orally or intraperitoneally administered 2 g of glucose solution per kg body weight and their blood glucose levels were measured (by tail nick) before (0 min) and after glucose challenge for 2 to 3 h.

DIO Study. DIO mice (C57BL/6, male, 25 weeks old, or 19 weeks on high fat diet) were randomized based on their body weight and were treated with daily subcutaneous injections of **O14** or vehicle (n = 5). Body weight and food intake were monitored daily throughout the study. At the end of the experiment, mice were sacrificed, and visceral fat mass was weighed. Collected plasma was used for cholesterol level determination according to the manufacturer's guide (cholesterol assay kit, Abcam, Cambridge, England) and triglyceride level using a triglyceride colorimetric assay kit (Cayman chemical, Ann Arbor, Michigan).

Oil Red Staining. Frozen tissue sections of liver were cut at 10 μm and air-dried onto slides. After fixation in 10% formalin for 5 min, the slides were briefly washed with running tap water for 10 min, followed by rinsing with 60% isopropanol. Subsequently, oil red O working solution (0.3% oil red O) was used to stain lipid for 15 min. Slides were again rinsed with 60% isopropanol, and then, nuclei were lightly stained with alum hematoxylin, followed by rinsing with distilled water, and mounted in glycerin jelly. Pictures were taken under a microscope.

CDAA-Induced NASH Mouse Model. Male C57BL/6 mice (n = 9 per group) from the Jackson Laboratory (Bar Harbor, ME; age 5 weeks) were maintained in a controlled environment (12 h light/dark cycle; temperature 21−22 °C; humidity 50 ± 10%). After 1 week of acclimation, mice were randomized into groups with ad libitum access to water and specialized diets: either choline-supplemented L-amino-acid-defined diet (CSAA, catalog #518754, Dyets Inc., Bethlehem, PA) or choline-deficient L-amino-acid-defined diet (CDAA; catalog #518743; Dyets Inc.) for 12 weeks of diet induction. Animals were randomized based on serum alanine aminotransferase (ALT), aspartate aminotransferase (AST), and body weight into treatment groups, and mice were treated daily either with vehicle (saline) or with Semaglutide (40 μg/kg) and **O14** (40 μg/kg) subcutaneously for 4 weeks. Body weights were recorded weekly throughout the study. At the end of the study, mice were sacrificed and bled to collect terminal serum sample and wet liver weight for further analyses.

Biochemical and Histological Analyses. Terminal serum analytes including ALT, AST, and ALP were determined by Alfa Wassermann Vet Axcel clinical analyzer. Hepatic triglycerides were measured in liver homogenates with a colorimetric triglyceride kit (Cayman Chemical). Paraformaldehyde-fixed liver were paraffin-embedded, sectioned, and stained with hematoxylin-eosin and Picro-Sirius red by HistoTox Laboratories (Boulder, CO). All histological assessment (steatosis, fibrosis scoring) were performed by a certified histopathologist blind to treatment (HistoTox Laboratories) based on classification outlined by Kleiner et al.[55]

■ ASSOCIATED CONTENT

Supporting Information

The Supporting Information is available free of charge at https://pubs.acs.org/doi/10.1021/acs.bioconjchem.0c00093.

Materials and general procedures, including characterization and analysis (PDF)

■ AUTHOR INFORMATION

Corresponding Authors

Peter G. Schultz − *Calibr at The Scripps Research Institute, La Jolla, California 92037, United States; Department of Chemistry, The Skaggs Institute for Chemical Biology, The Scripps Research Institute, La Jolla, California 92037, United States;* orcid.org/0000-0003-3188-1202; Email: wshen@scripps.edu

Weijun Shen − *Calibr at The Scripps Research Institute, La Jolla, California 92037, United States;* orcid.org/0000-0001-8388-729X; Email: schultz@scripps.edu

Authors

Peng-Yu Yang − *Calibr at The Scripps Research Institute, La Jolla, California 92037, United States; Department of Chemistry, The Skaggs Institute for Chemical Biology, The Scripps Research Institute, La Jolla, California 92037, United States;* orcid.org/0000-0001-7554-5281

Huafei Zou − *Calibr at The Scripps Research Institute, La Jolla, California 92037, United States*

Zaid Amso − *Calibr at The Scripps Research Institute, La Jolla, California 92037, United States*

Candy Lee − *Calibr at The Scripps Research Institute, La Jolla, California 92037, United States*
David Huang − *Calibr at The Scripps Research Institute, La Jolla, California 92037, United States*
Ashley K. Woods − *Calibr at The Scripps Research Institute, La Jolla, California 92037, United States*
Vân T. B. Nguyen-Tran − *Calibr at The Scripps Research Institute, La Jolla, California 92037, United States*

Complete contact information is available at:
https://pubs.acs.org/10.1021/acs.bioconjchem.0c00093

Author Contributions

[§]P.-Y.Y., H.Z., and Z.A. contributed equally.

Notes

The authors declare no competing financial interest.

■ ACKNOWLEDGMENTS

We thank Elizabeth Chao, Lance Sherwood, Vanessa Nunez, and Qiangwei Fu for technical support.

■ ABBREVIATIONS

OXM, oxyntomodulin; T2D, type 2 diabetes; GLP-1, glucagon-like peptide-1; GLP-1R, glucagon-like peptide-1 receptor; GCG, glucagon; GCGR, glucagon receptor; Ex-4, exendin-4; PYY, peptide YY; GIP, glucose-dependent insulintropic peptide; FGF, fibroblast growth factor; PPARγ, peroxisome proliferator-activated receptor gamma; cAMP, cyclic adenosine monophosphate; CRE, cAMP response element; DIO, diet-induced obesity; OGTT, oral glucose tolerance test; IPGTT, intraperitoneal glucose tolerance test; C_{max}, maximal plasma concentration; T_{max}, time of maximal concentration; $t_{1/2}$, half-time of elimination; *i.v.*, intravenous; *s.c.*, subcutaneous; PK, pharmacokinetic; PD, pharmacodynamic; ALT, alanine transaminase; AST, aspartate aminotransferase; ALP, alkaline phosphatase; CDAA, choline-deficient L-amino acid; CSAA, choline-supplemented L-amino acid; NASH, nonalcoholic steatohepatitis; NAFLD, nonalcoholic fatty liver disease.

■ REFERENCES

(1) Rodgers, R. J., Tschop, M. H., and Wilding, J. P. (2012) Anti-obesity drugs: past, present and future. *Dis. Models & Mech. 5*, 621−626.
(2) Sjostrom, L., Lindroos, A. K., Peltonen, M., Torgerson, J., Bouchard, C., Carlsson, B., Dahlgren, S., Larsson, B., Narbro, K., Sjostrom, C. D., et al. (2004) Lifestyle, diabetes, and cardiovascular risk factors 10 years after bariatric surgery. *N. Engl. J. Med. 351*, 2683−2693.
(3) Tschop, M. H., Finan, B., Clemmensen, C., Gelfanov, V., Perez-Tilve, D., Muller, T. D., and DiMarchi, R. D. (2016) Unimolecular polypharmacy for treatment of diabetes and obesity. *Cell Metab. 24*, 51−62.
(4) McGavigan, A. K., and Murphy, K. G. (2012) Gut hormones: the future of obesity treatment? *Br. J. Clin. Pharmacol. 74*, 911−919.
(5) Finan, B., Clemmensen, C., and Muller, T. D. (2015) Emerging opportunities for the treatment of metabolic diseases: Glucagon-like peptide-1 based multi-agonists. *Mol. Cell. Endocrinol. 418*, 42−54.
(6) Muller, T. D., Finan, B., Clemmensen, C., DiMarchi, R. D., and Tschop, M. H. (2017) The new biology and pharmacology of glucagon. *Physiol. Rev. 97*, 721−766.
(7) Brandt, S. J., Gotz, A., Tschop, M. H., and Muller, T. D. (2018) Gut hormone polyagonists for the treatment of type 2 diabetes. *Peptides 100*, 190−201.
(8) Frias, J. P., Nauck, M. A., Van, J., Kutner, M. E., Cui, X., Benson, C., Urva, S., Gimeno, R. E., Milicevic, Z., Robins, D., et al. (2018) Efficacy and safety of LY3298176, a novel dual GIP and GLP-1 receptor agonist, in patients with type 2 diabetes: a randomised, placebo-controlled and active comparator-controlled phase 2 trial. *Lancet 392*, 2180−2193.
(9) Madsbad, S. (2016) Review of head-to-head comparisons of glucagon-like peptide-1 receptor agonists. *Diabetes, Obes. Metab. 18*, 317−332.
(10) Marino, A. B., Cole, S. W., and Nuzum, D. S. (2014) Alternative dosing strategies for liraglutide in patients with type 2 diabetes mellitus. *Am. J. Health-Syst. Pharm. 71*, 223−226.
(11) Pi-Sunyer, X., Astrup, A., Fujioka, K., Greenway, F., Halpern, A., Krempf, M., Lau, D. C., le Roux, C. W., Violante Ortiz, R., Jensen, C. B., et al. (2015) A randomized, controlled trial of 3.0 mg of liraglutide in weight management. *N. Engl. J. Med. 373*, 11−22.
(12) O'Neil, P. M., Birkenfeld, A. L., McGowan, B., Mosenzon, O., Pedersen, S. D., Wharton, S., Carson, C. G., Jepsen, C. H., Kabisch, M., and Wilding, J. P. H. (2018) Efficacy and safety of semaglutide compared with liraglutide and placebo for weight loss in patients with obesity: a randomised, double-blind, placebo and active controlled, dose-ranging, phase 2 trial. *Lancet 392*, 637−649.
(13) Habegger, K. M., Heppner, K. M., Geary, N., Bartness, T. J., DiMarchi, R., and Tschop, M. H. (2010) The metabolic actions of glucagon revisited. *Nat. Rev. Endocrinol. 6*, 689−697.
(14) Schulman, J. L., Carleton, J. L., Whitney, G., and Whitehorn, J. C. (1957) Effect of glucagon on food intake and body weight in man. *J. Appl. Physiol. 11*, 419−421.
(15) Tan, T. M., Field, B. C. T., McCullough, K. A., Troke, R. C., Chambers, E. S., Salem, V., Gonzalez Maffe, J., Baynes, K. C. R., De Silva, A., Viardot, A., et al. (2013) Coadministration of glucagon-like peptide-1 during glucagon infusion in humans results in increased energy expenditure and amelioration of hyperglycemia. *Diabetes 62*, 1131−1138.
(16) Cegla, J., Troke, R. C., Jones, B., Tharakan, G., Kenkre, J., McCullough, K. A., Lim, C. T., Parvizi, N., Hussein, M., Chambers, E. S., et al. (2014) Coinfusion of low-dose GLP-1 and glucagon in man results in a reduction in food intake. *Diabetes 63*, 3711−3720.
(17) Pocai, A. (2012) Unraveling oxyntomodulin, GLP1's enigmatic brother. *J. Endocrinol. 215*, 335−346.
(18) Pocai, A. (2014) Action and therapeutic potential of oxyntomodulin. *Mol. Metab. 3*, 241−251.
(19) Parlevliet, E. T., Heijboer, A. C., Schroder-van der Elst, J. P., Havekes, L. M., Romijn, J. A., Pijl, H., and Corssmit, E. P. (2008) Oxyntomodulin ameliorates glucose intolerance in mice fed a high-fat diet. *Am. J. Physiol. Endocrinol. Metab. 294*, E142−E147.
(20) Shankar, S. S., Shankar, R. R., Mixson, L., Miller, D., Beals, C. R., Steinberg, H. O., and Kelley, D. E. (2013) Oxyntomodulin Has Significant Acute Glucoregulatory Effects in Non-Diabetic Humans. *Diabetes 62*, A512−A513.
(21) Pocai, A., Carrington, P. E., Adams, J. R., Wright, M., Eiermann, G., Zhu, L., Du, X. B., Petrov, A., Lassman, M. E., Jiang, G. Q., et al. (2009) Glucagon-Like Peptide 1/Glucagon Receptor Dual Agonism Reverses Obesity in Mice. *Diabetes 58*, 2258−2266.
(22) Day, J. W., Ottaway, N., Patterson, J. T., Gelfanov, V., Smiley, D., Gidda, J., Findeisen, H., Bruemmer, D., Drucker, D. J., Chaudhary, N., et al. (2009) A new glucagon and GLP-1 co-agonist eliminates obesity in rodents. *Nat. Chem. Biol. 5*, 749−757.
(23) Lao, J., Hansen, B. C., Dimarchi, R., and Pocai, A. (2013) Effect of GLP1R/GCGR Dual Agonist in Monkeys. *Diabetes 62*, A257−A257.
(24) Day, J. W., Gelfanov, V., Smiley, D., Carrington, P. E., Eiermann, G., Chicchi, G., Erion, M. D., Gidda, J., Thornberry, N. A., Tschop, M. H., et al. (2012) Optimization of co-agonism at GLP-1 and glucagon receptors to safely maximize weight reduction in DIO-rodents. *Biopolymers 98*, 443−450.
(25) Ambery, P., Parker, V. E., Stumvoll, M., Posch, M. G., Heise, T., Plum-Moerschel, L., Tsai, L. F., Robertson, D., Jain, M., Petrone, M., et al. (2018) MEDI0382, a GLP-1 and glucagon receptor dual agonist,

in obese or overweight patients with type 2 diabetes: a randomised, controlled, double-blind, ascending dose and phase 2a study. *Lancet 391*, 2607−2618.

(26) Ambery, P. D., Klammt, S., Posch, M. G., Petrone, M., Pu, W., Rondinone, C., Jermutus, L., and Hirshberg, B. (2018) MEDI0382, a GLP-1/glucagon receptor dual agonist, meets safety and tolerability endpoints in a single-dose, healthy-subject, randomized, Phase 1 study. *Br. J. Clin. Pharmacol. 84*, 2325−2335.

(27) Tillner, J., Posch, M. G., Wagner, F., Teichert, L., Hijazi, Y., Einig, C., Keil, S., Haack, T., Wagner, M., Bossart, M., et al. (2019) A novel dual glucagon-like peptide and glucagon receptor agonist SAR425899: Results of randomized, placebo-controlled first-in-human and first-in-patient trials. *Diabetes, Obes. Metab. 21*, 120−128.

(28) Cohen, M. A., Ellis, S. M., Le Roux, C. W., Batterham, R. L., Park, A., Patterson, M., Frost, G. S., Ghatei, M. A., and Bloom, S. R. (2003) Oxyntomodulin suppresses appetite and reduces food intake in humans. *J. Clin. Endocrinol. Metab. 88*, 4696−4701.

(29) Wynne, K., Park, A. J., Small, C. J., Meeran, K., Ghatei, M. A., Frost, G. S., and Bloom, S. R. (2006) Oxyntomodulin increases energy expenditure in addition to decreasing energy intake in overweight and obese humans: a randomised controlled trial. *Int. J. Obes. 30*, 1729−1736.

(30) Schjoldager, B. T. G., Baldissera, F. G. A., Mortensen, P. E., Holst, J. J., and Christiansen, J. (1988) Oxyntomodulin: a potential hormone from the distal gut. Pharmacokinetics and effects on gastric acid and insulin secretion in man. *Eur. J. Clin. Invest. 18*, 499−503.

(31) Druce, M. R., Minnion, J. S., Field, B. C. T., Patel, S. R., Shillito, J. C., Tilby, M., Beale, K. E. L., Murphy, K. G., Ghatei, M. A., and Bloom, S. R. (2009) Investigation of structure-activity relationships of oxyntomodulin (oxm) using oxm analogs. *Endocrinology 150*, 1712−1721.

(32) Kerr, B. D., Flatt, P. R., and Gault, V. A. (2010) (D-Ser2)Oxm[mPEG-PAL]: a novel chemically modified analogue of oxyntomodulin with antihyperglycaemic, insulinotropic and anorexigenic actions. *Biochem. Pharmacol. 80*, 1727−1735.

(33) Liu, Y. L., Ford, H. E., Druce, M. R., Minnion, J. S., Field, B. C. T., Shillito, J. C., Baxter, J., Murphy, K. G., Ghatei, M. A., and Bloom, S. R. (2010) Subcutaneous oxyntomodulin analogue administration reduces body weight in lean and obese rodents. *Int. J. Obes. 34*, 1715−1725.

(34) Santoprete, A., Capitò, E., Carrington, P. E., Pocai, A., Finotto, M., Langella, A., Ingallinella, P., Zytko, K., Bufali, S., Cianetti, S., et al. (2011) DPP-IV-resistant, long-acting oxyntomodulin derivatives. *J. Pept. Sci. 17*, 270−280.

(35) Henderson, S. J., Konkar, A., Hornigold, D. C., Trevaskis, J. L., Jackson, R., Fritsch Fredin, M., Jansson-Lofmark, R., Naylor, J., Rossi, A., Bednarek, M. A., et al. (2016) Robust anti-obesity and metabolic effects of a dual GLP-1/glucagon receptor peptide agonist in rodents and non-human primates. *Diabetes, Obes. Metab. 18*, 1176−1190.

(36) Valdecantos, M. P., Pardo, V., Ruiz, L., Castro-Sanchez, L., Lanzon, B., Fernandez-Millan, E., Garcia-Monzon, C., Arroba, A. I., Gonzalez-Rodriguez, A., Escriva, F., et al. (2017) A novel glucagon-like peptide 1/glucagon receptor dual agonist improves steatohepatitis and liver regeneration in mice. *Hepatology (Hoboken, NJ, U. S.) 65*, 950−968.

(37) Lau, J., Bloch, P., Schaffer, L., Pettersson, I., Spetzler, J., Kofoed, J., Madsen, K., Knudsen, L. B., McGuire, J., Steensgaard, D. B., et al. (2015) Discovery of the once-weekly glucagon-like peptide-1 (GLP-1) analogue semaglutide. *J. Med. Chem. 58*, 7370−7380.

(38) Claus, T. H., Pan, C. Q., Buxton, J. M., Yang, L., Reynolds, J. C., Barucci, N., Burns, M., Ortiz, A. A., Roczniak, S., Livingston, J. N., et al. (2007) Dual-acting peptide with prolonged glucagon-like peptide-1 receptor agonist and glucagon receptor antagonist activity for the treatment of type 2 diabetes. *J. Endocrinol. 192*, 371−380.

(39) Bianchi, E., Carrington, P. E., Ingallinella, P., Finotto, M., Santoprete, A., Petrov, A., Eiermann, G., Kosinski, J., Marsh, D. J., Pocai, A., et al. (2013) A PEGylated analog of the gut hormone oxyntomodulin with long-lasting antihyperglycemic, insulinotropic and anorexigenic activity. *Bioorg. Med. Chem. 21*, 7064−7073.

(40) Zhou, J., Cai, X., Huang, X., Dai, Y., Sun, L., Zhang, B., Yang, B., Lin, H., Huang, W., and Qian, H. (2017) A novel glucagon-like peptide-1/glucagon receptor dual agonist exhibits weight-lowering and diabetes-protective effects. *Eur. J. Med. Chem. 138*, 1158−1169.

(41) Yang, P.-Y., Zou, H., Chao, E., Sherwood, L., Nunez, V., Keeney, M., Ghartey-Tagoe, E., Ding, Z., Quirino, H., Luo, X., et al. (2016) Engineering a long-acting, potent GLP-1 analog for microstructure-based transdermal delivery. *Proc. Natl. Acad. Sci. U. S. A. 113*, 4140−4145.

(42) Lear, S., Amso, Z., and Shen, W. (2019) Engineering PEG-fatty acid stapled, long-acting peptide agonists for G protein-coupled receptors, *Methods in enzymology* (Shukla, A. K., Ed.) pp 183−200, Chapter 8, Vol. *622*, Academic Press.

(43) Yang, P. Y., Zou, H., Lee, C., Muppidi, A., Chao, E., Fu, Q., Luo, X., Wang, D., Schultz, P. G., and Shen, W. (2018) Stapled, long-acting glucagon-like peptide 2 analog with efficacy in dextran sodium sulfate induced mouse colitis models. *J. Med. Chem. 61*, 3218−3223.

(44) Runge, S., Thogersen, H., Madsen, K., Lau, J., and Rudolph, R. (2008) Crystal structure of the ligand-bound glucagon-like peptide-1 receptor extracellular domain. *J. Biol. Chem. 283*, 11340−11347.

(45) Siu, F. Y., He, M., de Graaf, C., Han, G. W., Yang, D. H., Zhang, Z. Y., Zhou, C. H., Xu, Q. P., Wacker, D., Joseph, J. S., et al. (2013) Structure of the human glucagon class B G-protein-coupled receptor. *Nature 499*, 444.

(46) Muppidi, A., Zou, H., Yang, P. Y., Chao, E., Sherwood, L., Nunez, V., Woods, A. K., Schultz, P. G., Lin, Q., and Shen, W. (2016) Design of potent and proteolytically stable oxyntomodulin analogs. *ACS Chem. Biol. 11*, 324−328.

(47) Parks, J. S., Cistola, D. P., Small, D. M., and Hamilton, J. A. (1983) Interactions of the carboxyl group of oleic acid with bovine serum albumin: a 13C NMR study. *J. Biol. Chem. 258*, 9262−9269.

(48) Bhattacharya, A. A., Grune, T., and Curry, S. (2000) Crystallographic analysis reveals common modes of binding of medium and long-chain fatty acids to human serum albumin. *J. Mol. Biol. 303*, 721−32.

(49) Knudsen, L. B., and Lau, J. (2019) The discovery and development of liraglutide and semaglutide. *Front. Endocrinol. 10*, 1 DOI: 10.3389/fendo.2019.00155.

(50) Salem, V., Izzi-Engbeaya, C., Coello, C., Thomas, D. B., Chambers, E. S., Comninos, A. N., Buckley, A., Win, Z., Al-Nahhas, A., Rabiner, E. A., et al. (2016) Glucagon increases energy expenditure independently of brown adipose tissue activation in humans. *Diabetes, Obes. Metab. 18*, 72−81.

(51) Habegger, K. M., Stemmer, K., Cheng, C., Müller, T. D., Heppner, K. M., Ottaway, N., Holland, J., Hembree, J. L., Smiley, D., Gelfanov, V., et al. (2013) Fibroblast growth factor 21 mediates specific glucagon actions. *Diabetes 62*, 1453−1463.

(52) Patel, V., Joharapurkar, A., Kshirsagar, S., Patel, M., Sutariya, B., Patel, H., Pandey, D., Patel, D., Ranvir, R., Kadam, S., et al. (2018) Coagonist of glucagon-like peptide-1 and glucagon receptors ameliorates nonalcoholic fatty liver disease. *Can. J. Physiol. Pharmacol. 96*, 587−596.

(53) More, V. R., Lao, J., McLaren, D. G., Cumiskey, A. M., Murphy, B. A., Chen, Y., Previs, S., Stout, S., Patel, R., Satapati, S., et al. (2017) Glucagon like receptor 1/ glucagon dual agonist acutely enhanced hepatic lipid clearance and suppressed de novo lipogenesis in mice. *PLoS One 12*, No. e0186586.

(54) Hansen, H. H., Feigh, M., Veidal, S. S., Rigbolt, K. T., Vrang, N., and Fosgerau, K. (2017) Mouse models of nonalcoholic steatohepatitis in preclinical drug development. *Drug Discovery Today 22*, 1707−1718.

(55) Kleiner, D. E., Brunt, E. M., Van Natta, M., Behling, C., Contos, M. J., Cummings, O. W., Ferrell, L. D., Liu, Y. C., Torbenson, M. S., Unalp-Arida, A., et al. (2005) Design and validation of a histological scoring system for nonalcoholic fatty liver disease. *Hepatology (Hoboken, NJ, U. S.) 41*, 1313−1321.

https://dx.doi.org/10.1021/acs.bioconjchem.0c00093
Bioconjugate Chem. XXXX, XXX, XXX−XXX